

## Southern coastal system of the San Jorge Gulf during spring

REGINA PIERATTINI-MARTINEZ<sup>1,2</sup>; JUAN P. PISONI<sup>1,2</sup> & FLAVIO E. PAPARAZZO<sup>1,2</sup>✉

<sup>1</sup>Centro para el Estudio de Sistemas Marinos, CESIMAR-CONICET. <sup>2</sup>Instituto Patagónico del Mar, IPaM-UNPSJB.

**ABSTRACT.** The San Jorge Gulf was declared an area of national economic, commercial, conservation and diversity interest. To contribute to its study, the southern coastal sector of the gulf was characterised in physical and chemical parameters in spring campaigns (November 2016 and 2017). Samples were taken on board the oceanographic vessel Puerto Deseado in three perpendicular to the coast transects and another one to the southeast of the gulf, which crosses a thermohaline front. The perpendicular to the coast transects showed a similar pattern of distribution of physical and chemical properties in the water column. At nearshore stations, the water column was homogeneous and the nutrient concentrations between the surface and bottom layers were similar. At offshore stations, the water column was stratified and the nutrient concentrations were higher near the bottom than at surface. In 2016, a wind induced upwelling front was observed in the southwest of the gulf. Both sides of the thermohaline front did not show significant chemical differences. Throughout the study area, silicic acid and nitrate limited primary production. Satellite chlorophyll-*a* data and fluorescence profiles showed that the southern sector of the gulf has a high biomass of phytoplankton during November. We conclude that the southern sector of the SJG has different features depending on the external forcing caused by the front. The presence of fronts stimulates the growth of phytoplankton biomass through the injection of nutrients from the homogeneous part to the stratified sector. This would affect phytoplankton community and, thus, the productivity of the system.

[Keywords: fronts, macronutrients, biological production, upwelling, San Jorge Gulf]

**RESUMEN. Sistema costero del sur del Golfo San Jorge durante la primavera.** El Golfo San Jorge fue declarado zona de interés económico, comercial, de conservación y de diversidad nacional. Para contribuir a su estudio, se caracterizó el sector costero sur del golfo en parámetros físicos y químicos en campañas de primavera (noviembre de 2016 y 2017). Se tomaron muestras a bordo del buque oceanográfico Puerto Deseado en tres transectas perpendiculares a la costa y en otra al sureste del golfo, que atraviesa un frente termohalino. Las transectas perpendiculares a la costa mostraron un patrón similar de distribución de las propiedades físicas y químicas en la columna de agua. En las estaciones cercanas a la costa, la columna de agua fue homogénea y las concentraciones de nutrientes entre las capas de superficie y fondo fueron similares. En las estaciones alejadas de la costa, la columna de agua estuvo estratificada y las concentraciones de nutrientes fueron mayores en la capa de fondo que en la superficie. En 2016 se observó un frente de surgencia por viento en el suroeste del golfo. No se observaron diferencias químicas significativas a ambos lados del frente termohalino. En toda el área de estudio, el ácido silícico y el nitrato limitaron la producción primaria. Los datos satelitales de clorofila-*a* y los perfiles de fluorescencia mostraron que el sector sur del golfo presenta una elevada biomasa de fitoplancton durante el mes de noviembre. Concluimos que el sector sur del GSJ presenta diferentes características en función del forzamiento externo que origina el frente. La presencia de frentes estimula el crecimiento de la biomasa fitoplanctónica a través de la inyección de nutrientes desde el sector homogéneo al estratificado. Esto afectaría a las comunidades de fitoplancton y, por lo tanto, a la productividad del sistema.

[Palabras clave: frentes, macronutrientes, producción biológica, surgencia, Golfo San Jorge]

## INTRODUCTION

An ocean front is an area where abrupt horizontal changes of different water properties and characteristics are observed (Guerrero and Piola 1997; Paparazzo 2003; Rivas and Pisoni 2010). The main properties studied to indicate the presence of fronts are temperature and salinity (Acha et al. 2015). In addition, remote sensing is a useful tool for studying frontal systems (Belkin and O'Reilly 2009) by estimating variables such as sea surface temperature (SST) and chlorophyll-*a* (Chl-*a*). Furthermore, Chl-*a* alongside with fluorescence are commonly used as proxy indicators of phytoplankton biomass and these primary producers are the base of the food chain. Olson (2002) and Bianchi et al. (2009) suggest that biological responses at fronts are related to the sensitivity of the ecosystem to vertical movements. Vertical mixing (homogenization of the water column generated by ascending and descending movements) affects stratification by breaking the layer structure and environmental characteristics of the upper sea layer. Thus, environmental variations related to the depth of the mixing layer, euphotic depth and nutrient supply encourage primary production and allow phytoplankton development (Flores-Melo et al. 2018). These conditions for the development and permanence of organisms could be altered differently on both sides of the fronts (Bianchi et al. 2005).

Nitrite ( $\text{NO}_2^-$ ), nitrate ( $\text{NO}_3^-$ ), ammonium ( $\text{NH}_4^+$ ), phosphate ( $\text{PO}_4^{3-}$ ) and silicic acid ( $\text{Si}(\text{OH})_4$ ) are essential nutrients for the development of phytoplankton in aqueous systems. Due to the importance of nutrients in marine systems, measurements of nutrient concentrations are among the most commonly performed analyses in oceanographic research. For example, Redfield (1934) found that, regardless of absolute concentration, the C:N:P ratio in the sea is constant and equal to C:N:P=106:16:1. Brzenziski (1985), due to the relationship of Silica with diatoms, added Si to this ratio (C:Si:N:P=106:15:16:1). This relationship between nutrients allows one to estimate one nutrient from another and to know if there is any input or differential uptake of any nutrient. However, when the water column is stratified, the nutrients in the upper layer are consumed by the primary producers, depleting them or reducing their concentration to such low values that they limit their development ( $\text{NO}_3^- < 0.7 \mu\text{M}$ ,  $\text{PO}_4^{3-} < 0.3 \mu\text{M}$  and  $\text{Si}(\text{OH})_4 < 1.8 \mu\text{M}$ ) (Millero 2013) and

change this ratio. In this way, the analysis of nutrient concentration explains the influence of fronts on chemical compounds (nutrients), which, in turn, explains the relevance for primary producers.

Laurs et al. (1984) and Yañez et al. (1996) describe that there is a strong relationship between aggregations of pelagic fish and environmental variables. Likewise, Svendsen et al. (2020) suggested that fronts may influence marine fish assemblages. In addition, Williams et al. (2010) studying the common hake in the San Matías Gulf (Argentina) found that fishing production is greater where the thermal front is present, suggesting the biological relevance of the oceanographic structure. Therefore, in order to fully understand the environment in which ocean fronts are found, it is important to link the physical, chemical and biological processes that occur in them.

Several frontal systems have been detected in the San Jorge Gulf (SJG) (Glembocki et al. 2015) (Figure 1). In addition, the southern area of the SJG is one of the areas with highest productivity in the world (Costanza et al. 1997; Góngora et al. 2012) and it is also relevant for shrimp (*Pleoticus muelleri*, Bate, 1888) and hake resources (*Merluccius hubbsi*, Marini, 1933), two of the main commercial species in the gulf (Fernández et al. 2007; Góngora et al. 2012), since the highest individuals concentrations that support such fisheries are located there (Fernández et al. 2007). For this reason, the goal of this study is to characterize the physical and chemical conditions of the water column during spring in the south of the SJG and its association with temperature and Chl-*a* concentration observed by remote sensors.

## MATERIALS AND METHODS

### *Study area*

The SJG is located in the Argentine coastal sector from Dos Bahías Cape (44°55' S - 65°32' W) to Tres Puntas Cape (47°06' S - 65°52' W) (Figure 1), encompassing more than 39000 km<sup>2</sup> of surface. The deepest sector of the gulf (~110 m) is located in the central region and decrease towards the coasts. In the southern sector, a thermohaline tidal front has been observed, with seasonal and spatial variability (Rivas and Pisoni 2010; Carbajal et al. 2018; Flores-Melo et al. 2018). On the other hand, an upward movement of water on the coast (coastal upwelling) has been observed in the south-western sector due to the intense

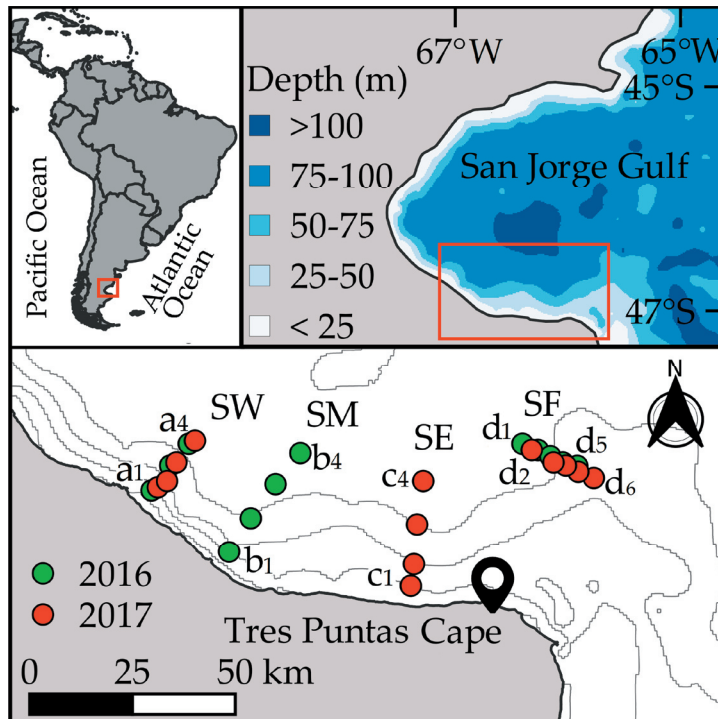


**Figure 1.** Geographical location of the sampling stations. Green: 2016. Red: 2017. The shades of blue represent the depth (m). SW: Southwest transect. SM: South middle transect. SE: Southeast transect. SF: Transect crossing a front located southeast of the gulf. **Figura 1.** Localización geográfica de las estaciones de muestreo. Verde: 2016. Rojo: 2017. Las tonalidades de azul representan la profundidad (m). SW: Transecta suroeste. SM: Transecta sur medio. SE: Transecta sureste. SF: Transecta que cruza el frente localizado al sur del golfo.

winds in the region (Pisoni et al. 2020). This upwelling was previously predicted from models (Tonini et al. 2006; Matano and Palma 2018), and as a consequence, an increase in primary productivity was observed (Paparazzo et al. 2021).

#### Sampling

The sampling was carried out within the framework of the Golfo San Jorge Working Group of Pampa Azul initiative, on board the Oceanographic Vessel Puerto Deseado, in the south of the SJG (Figure 1), during two austral spring campaigns (November 2016 and 2017). Two transects perpendicular to the coast were made each year. The southwest transect (SW) and the southern middle transect (SM) were carried out in 2016, while the southwest transect (SW) and the southeast transect (SE) were carried out in 2017. Additionally, a transect crossing a front located southeast of the gulf (SF) was made in both years (Figure 1).

Seawater samples were collected for macronutrients analysis (nitrate ( $\text{NO}_3^-$ ), nitrite ( $\text{NO}_2^-$ ), phosphate ( $\text{PO}_4^{3-}$ ) and silicic acid ( $\text{Si}(\text{OH})_4$ ). At each station, water samples were taken at the surface (5 m depth), at the depth of the maximum fluorescence (~25 m depth), immediately below the pycnocline (layer in which the density vary abruptly in a few meters in the water column) and near the

bottom (~5 m depth), using an oceanographic rosette system with 12 Niskin General Oceanic® bottles (5 L). Temperature, salinity, density and fluorescence's vertical profiles were obtained using a CTD Sea Bird 911® and a fluorometer Sea Point®, both attached to the rosette. As soon as they arrived on deck, pH values of each bottle were recorded through a pHmeter Yokogawa®. Water samples for nutrient determination were taken in duplicate. They were stored in 125 mL of acid-clean plastic bottles and kept frozen at  $-20^\circ\text{C}$  until analysis in the laboratory on land.

#### Sample analysis

Macronutrient analysis ( $\text{NO}_3^-$ ,  $\text{NO}_2^-$ ,  $\text{PO}_4^{3-}$  and  $\text{Si}(\text{OH})_4$ ) were performed by colorimetric methods using an Skalar San Plus® autoanalyzer (Skalar Analytical V. B. 2005a,b,c). The precision of measurements for  $\text{NO}_3^-$ ,  $\text{PO}_4^{3-}$  and  $\text{Si}(\text{OH})_4$  was 0.03, 0.02 and 0.06  $\mu\text{M}$  respectively. Since the  $\text{NO}_2^-$  concentration was low ( $<0.3 \mu\text{M}$ ), in this work  $\text{NO}_3^- + \text{NO}_2^-$  is expressed as  $\text{NO}_3^-$ .

#### Sea surface temperature and chlorophyll-a satellite data

In order to corroborate the presence and position of the front and to obtain an estimation of the phytoplankton biomass, SST and Chl-*a* data from monthly mean (November) sea surface images were obtained. Satellite images

with a spatial resolution of 4 km<sup>2</sup>, captured through the Moderate Resolution Imaging Spectroradiometer (MODIS) sensor, installed on board the Aqua satellite of the United States National Aerospace Administration (NASA), are freely accessible on the Web interface of NASA Giovanni (giovanni.gsfc.nasa.gov).

*Data analysis*

For plotting macronutrients, temperature, salinity, density (sigma-t) and fluorescence profiles, the Surfer 12<sup>®</sup> software (Kriging method for data interpolation) was used. Bathymetry shown in Figure 2 was estimated from the data obtained by the CTD. In this

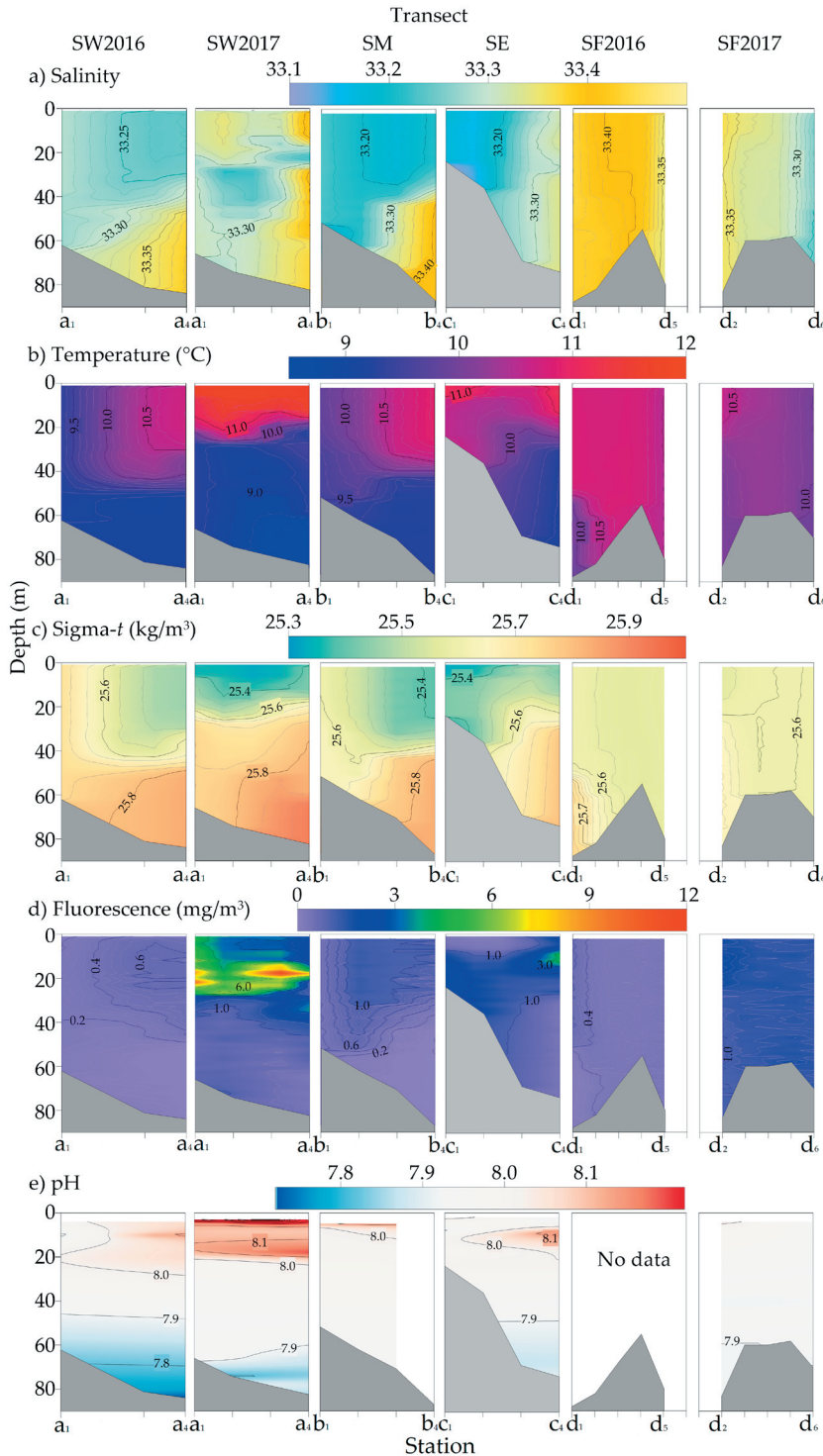


**Figure 2.** Vertical profiles along the transects. a) Salinity. b) Temperature. c) Sigma-t. d) Fluorescence. e) pH. See sampling locations in Figure 1. SW: Southwest transect. SM: South middle transect. SE: Southeast transect. SF: Transect crossing a front located southeast of the gulf.

**Figura 2.** Perfiles verticales a lo largo de las transectas. a) Salinidad. b) Temperatura. c) Sigma-t. d) Fluorescencia. e) pH. Ver localizaciones de muestreo en la Figura 1. SW: Transecta suroeste. SM: Transecta sur medio. SE: Transecta sureste. SF: Transecta que cruza el frente localizado al sur del golfo.

study, the values of  $\text{NO}_3^- < 0.7 \mu\text{M}$ ,  $\text{PO}_4^{3-} < 0.3 \mu\text{M}$  and  $\text{Si}(\text{OH})_4 < 1.8 \mu\text{M}$  values were considered limiting for primary producers according to Millero (2013). Macronutrients ratios  $\text{NO}_3^-/\text{PO}_4^{3-}$ ,  $\text{Si}(\text{OH})_4/\text{PO}_4^{3-}$  and  $\text{Si}(\text{OH})_4/\text{NO}_3^-$  were interpreted according to Brzezinski (1985). In order to analyse the degree of relationship between the variables, a bivariate correlation analysis was performed following Pearson's correlation. Georeferenced images were performed using Qgis (qgis.org).

## RESULTS

Physical properties in the water column showed a similar distribution pattern along the transects perpendicular to the coast (Figure 2) (SW 2016, SM and SE, except SW 2017). At the near-shore stations ( $a_1$ ,  $b_1$ ,  $c_1$ , and  $c_2$ ), salinity ( $33.23 \pm 0.05$ ), temperature ( $9.8 \pm 0.6 \text{ }^\circ\text{C}$ ), density ( $25.59 \pm 0.14 \text{ kg/m}^3$ ) and fluorescence ( $< 1 \text{ mg/m}^3$ ) showed homogeneous values in a non-stratified water column. On the other hand, the sampling stations far from the coast (all the remaining sampling stations along the transects) showed a stratified water column that varied in magnitude and depth depending on the transect. In the mixing layer ( $< 40 \text{ m}$  depth), the water was warmer ( $> 10.3 \text{ }^\circ\text{C}$ ), less saline ( $< 33.25$ ) and, therefore, less dense ( $< 25.51 \text{ kg/m}^3$ ); 5 m above the bottom the water was cooler ( $< 10.0 \text{ }^\circ\text{C}$ ), saltier ( $> 33.35$ ) and denser ( $> 25.60 \text{ kg/m}^3$ ). At these sampling stations, the highest fluorescence values ( $> 2 \text{ mg/m}^3$ ) were found between 10 and 25 m above the pycnocline. These estimates were coincident with the highest pH values (7.83 and 8.10). Satellite data for SST (Figure 3) suggest a similar distribution pattern for both years (Figure 2b). The highest temperatures were found in the central part of the gulf, while the lowest temperatures were found on the coast and towards the interior of the shelf. In addition, in 2016—but not in 2017—an upwelling of cold water was observed in the SW transect.

A low-salinity water intrusion ( $< 33.25$ ) between 20 and 40 m depth was observed in the SW transect conducted in 2017 (Figure 2) (SW 2017). It also showed thermal ( $2.36 \text{ }^\circ\text{C}$ ) and density ( $0.25 \text{ kg/m}^3$ ) stratification at 9 m. The pycnocline were located in the vicinity of 20 m depth. Above pycnocline, the fluorescence values were high ( $> 2 \text{ mg/m}^3$ ), reaching a maximum value of  $12.09 \text{ mg/m}^3$ , coinciding with the highest pH values.

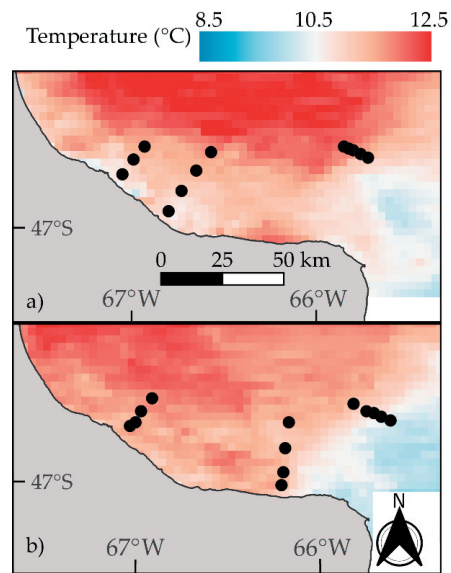


**Figure 3.** Distribution of sea surface temperature ( $^\circ\text{C}$ ) south of the SJG. a) November 2016. b) November 2017. Data ( $4 \text{ km}^2$  of spatial resolution) were obtained from the official Giovanni NASA site (giovanni.gsfc.nasa.gov).

**Figura 3.** Distribución de temperatura superficial del mar ( $^\circ\text{C}$ ) al sur del GSJ. a) Noviembre de 2016. b) Noviembre de 2017. Los datos ( $4 \text{ km}^2$  de resolución espacial) fueron obtenidos del sitio oficial de Giovanni NASA (giovanni.gsfc.nasa.gov).

In the SF transect, a similar pattern of distribution was found but different values of physical variables for both years (Figure 2) (SF 2016 and SF 2017). The water column at the first sampling station ( $d_1$  in 2016 and  $d_2$  in 2017 in Figure 1, the innermost of the gulf) showed a weak stratification, while in the next stations the water column was homogeneous. Salinity was higher in 2016 (33.39 to 33.44) than in 2017 (33.25 to 33.37), and thermal stratification was stronger in 2016 ( $0.91 \text{ }^\circ\text{C}$  in 14 m) than in 2017 ( $0.39 \text{ }^\circ\text{C}$  in 16 m), when a weak bottom front was detected (see Figure 2b). Satellite data for monthly SST (Figure 3) showed a SST gradient in 2017 ( $0.05 \text{ }^\circ\text{C/km}$ ), in agreement with Figure 2b. In addition, a lower SST gradient ( $0.03 \text{ }^\circ\text{C/km}$ ) was observed in 2016. Despite these differences, the density was similar in both years (2016:  $25.60 \pm 0.05 \text{ kg/m}^3$ ; 2017:  $25.61 \pm 0.02 \text{ kg/m}^3$ ). Fluorescence showed low values, being lower in 2016 ( $0.30 \pm 0.14 \text{ mg/m}^3$ ) than in 2017 ( $1.38 \pm 0.23 \text{ mg/m}^3$ ). During 2016 pH values were not recorded, while in 2017 pH showed homogeneous values (7.9–8.01) with an increase on the surface of the innermost stations.

Macronutrients concentration varied with depth (Figure 4) and water column stability.

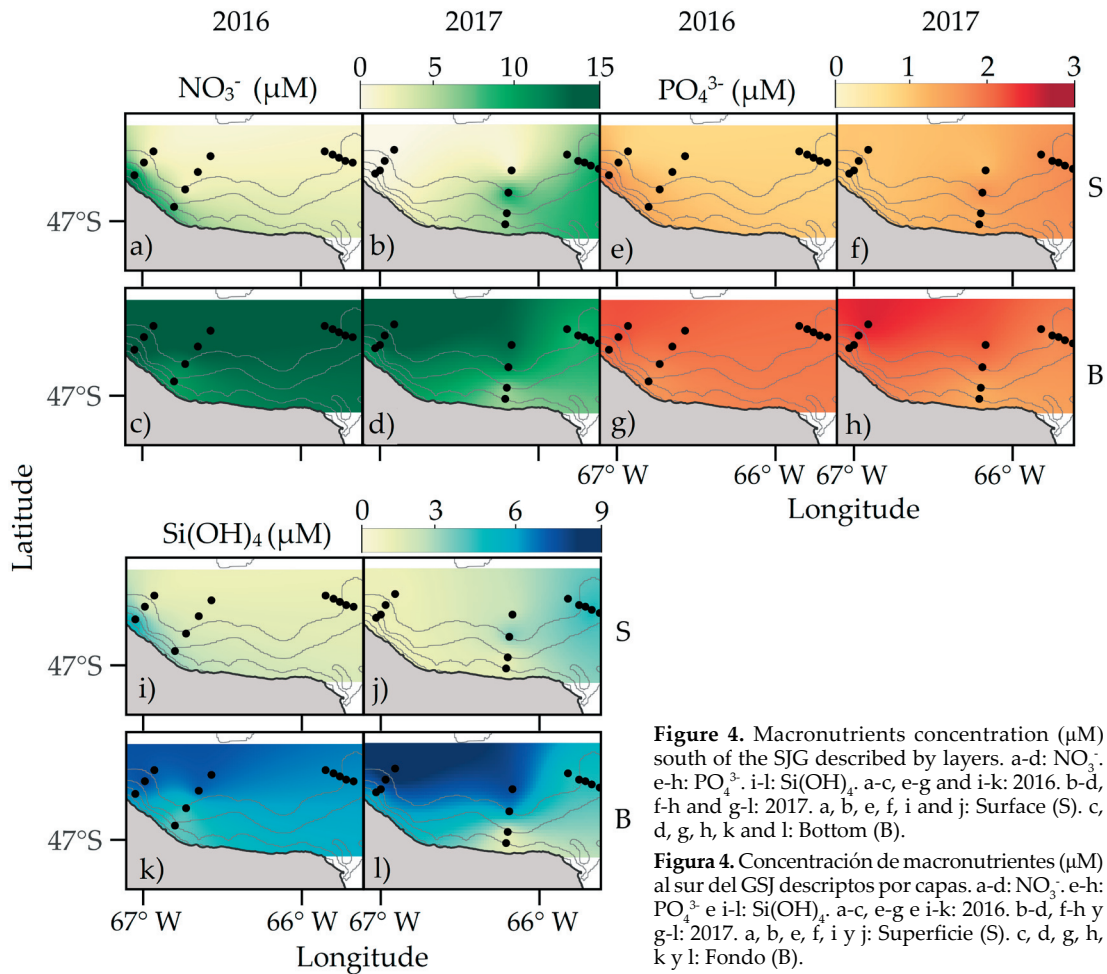


**Figure 4.** Macronutrients concentration ( $\mu\text{M}$ ) south of the SJG described by layers. a-d:  $\text{NO}_3^-$ . e-h:  $\text{PO}_4^{3-}$ . i-l:  $\text{Si(OH)}_4$ . a-c, e-g and i-k: 2016. b-d, f-h and g-l: 2017. a, b, e, f, i and j: Surface (S). c, d, g, h, k and l: Bottom (B).

**Figura 4.** Concentración de macronutrientes ( $\mu\text{M}$ ) al sur del GSJ descritos por capas. a-d:  $\text{NO}_3^-$ . e-h:  $\text{PO}_4^{3-}$ . e i-l:  $\text{Si(OH)}_4$ . a-c, e-g e i-k: 2016. b-d, f-h y g-l: 2017. a, b, e, f, i y j: Superficie (S). c, d, g, h, k y l: Fondo (B).

Near the bottom, the  $\text{NO}_3^-$ ,  $\text{PO}_4^{3-}$  and  $\text{Si(OH)}_4$  concentrations increase off-shore, while the surface concentration decrease in that direction. Near shore stations ( $a_1$ ,  $b_1$ ,  $c_1$  and  $c_2$ ), with a homogeneous water column, showed higher concentrations in 2016 ( $\text{NO}_3^- \sim 10.67 \mu\text{M}$ ;  $\text{PO}_4^{3-} \sim 1.60 \mu\text{M}$  and  $\text{Si(OH)}_4 \sim 4.43 \mu\text{M}$ )

than in 2017 ( $\text{NO}_3^- \sim 5.60 \mu\text{M}$ ;  $\text{PO}_4^{3-} \sim 1.35 \mu\text{M}$  and  $\text{Si(OH)}_4 \sim 2.46 \mu\text{M}$ ) (Table 1). The offshore stations ( $a_2$ - $a_4$ ,  $b_2$ - $b_4$ ,  $c_3$ - $c_4$  and  $d_1$ - $d_6$ ), with a stratified water column, showed a higher concentration of nutrients near the bottom than at the surface. In addition, the nutrients concentration near the bottom was higher in

**Table 1.** Average concentration ( $\mu\text{M}$ )  $\pm$  standard deviation. C: Coastal station ( $a_1$ ,  $b_1$  and  $c_1$ ). NC: Non-coastal station (rest of stations). S: Surface. B: Bottom.

**Tabla 1.** Concentración promedio ( $\mu\text{M}$ )  $\pm$  desvío estándar. C: Estación costera ( $a_1$ ,  $b_1$  y  $c_1$ ). NC: Estación no costera (resto de estaciones). S: Superficie. B: Fondo.

|      |   | $\text{NO}_3^-$ ( $\mu\text{M}$ ) | $\text{PO}_4^{3-}$ ( $\mu\text{M}$ ) | $\text{Si(OH)}_4$ ( $\mu\text{M}$ ) |
|------|---|-----------------------------------|--------------------------------------|-------------------------------------|
| 2016 |   |                                   |                                      |                                     |
| C    | S | 9.3 $\pm$ 3.4                     | 1.5 $\pm$ 0.4                        | 3.8 $\pm$ 1.6                       |
|      | B | 11.8 $\pm$ 2.8                    | 1.8 $\pm$ 0.2                        | 5.0 $\pm$ 1.7                       |
| NC   | S | 1.8 $\pm$ 0.4                     | 1.0 $\pm$ 0.1                        | 1.6 $\pm$ 0.2                       |
|      | B | 13.9 $\pm$ 1.5                    | 2.0 $\pm$ 0.2                        | 6.3 $\pm$ 1.5                       |
| 2017 |   |                                   |                                      |                                     |
| C    | S | 2.8 $\pm$ 2.9                     | 1.1 $\pm$ 0.3                        | 1.2 $\pm$ 0.3                       |
|      | B | 8.4 $\pm$ 4.0                     | 1.6 $\pm$ 0.4                        | 3.7 $\pm$ 3.2                       |
| NC   | S | 4.9 $\pm$ 3.9                     | 1.4 $\pm$ 0.3                        | 2.8 $\pm$ 1.5                       |
|      | B | 10.6 $\pm$ 3.0                    | 1.9 $\pm$ 0.3                        | 5.5 $\pm$ 2.3                       |

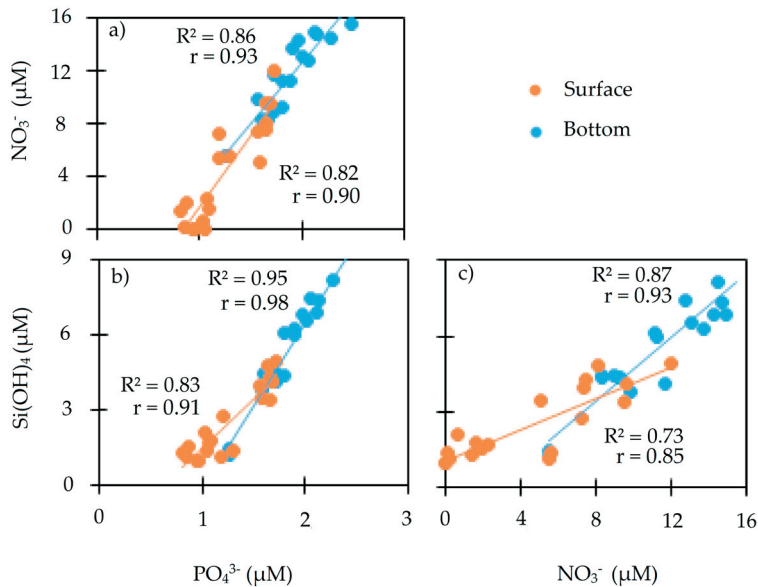


**Figure 5.** Linear regression between the macronutrients concentration at the surface layer south of the SJG. a) P vs. N. b) P vs. Si. c) N vs. Si. Light blue: Bottom. Orange: Surface.

**Figura 5.** Regresión lineal entre la concentración de macronutrientes de la capa de superficie al sur del GSJ. a) P vs. N. b) P vs. Si. c) N vs. Si. Celeste: Fondo. Naranja: Superficie.

2016 than in 2017, while the opposite occurs at surface (Figure 4, and NC in Table 1).

The average Si:N:P ratio of the southern sector of the SJG was 5.13:10.66:1. The N:P and Si:P ratios near the bottom (~10.61 and ~6.62, respectively) were higher than those at the surface (~9.27 and ~3.91, respectively) (Figure 5), showing that N and Si concentration tends to increase with depth more than P. Regarding the Si:N ratio, at surface the values (~0.63) were higher than near the bottom (~0.31). It is important to note that this ratio in the SW transect (2017) was high (>10) in almost all stations.

Results showed an inversely linear relationship between temperature and macronutrients concentration (Figure 6). High nutrient concentration was associated with low temperature. However, the relationship was different for each nutrient and each layer analysed, obtaining a better relationship near the bottom layer than at surface.

Based on remotely estimated Chl-*a*, the surface concentration in this sector of the SJG in November ranged between 1.16 and 7.52 mg/m<sup>3</sup> (Figure 7). The lowest values were recorded in the eastern region of the gulf (2016: <5.7 mg/m<sup>3</sup>; 2017: <2.1 mg/m<sup>3</sup>). On the other hand, the highest values were recorded towards the southwestern sector of the gulf, differing in distribution and magnitude between the two years under study. In 2016, the highest values were observed around the SM transect (>3.65 mg/m<sup>3</sup>), while in 2017, the highest values were observed to the west of the SW transect (>4.32 mg/m<sup>3</sup>).

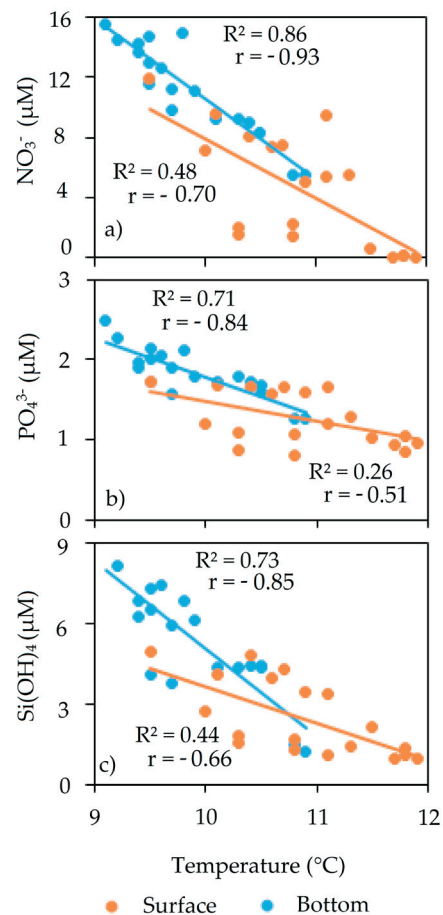


**Figure 6.** Linear regression between macronutrients concentration and temperature south of the SJG. a) N. b) P. c) Si. Light blue: Bottom. Orange: Surface.

**Figura 6.** Regresión lineal entre la concentración de macronutrientes y la temperatura al sur del GSJ. a) N. b) P. c) Si. Celeste: Fondo. Naranja: Superficie.

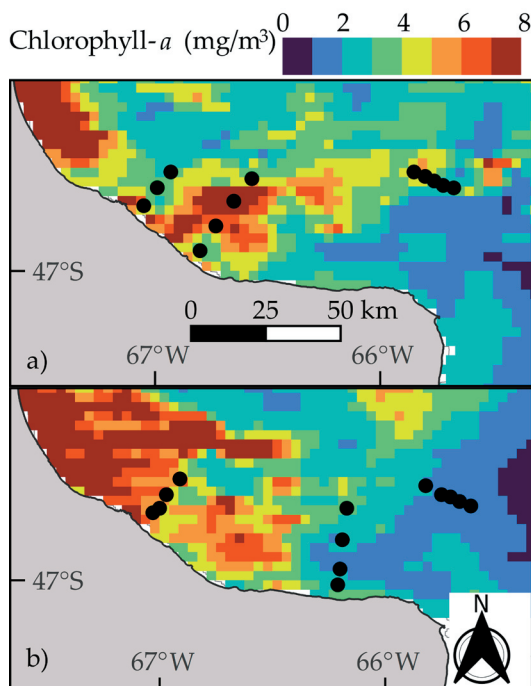


**Figure 7.** Distribution of Chl-*a* ( $\text{mg}/\text{m}^3$ ) south of the SJG. a) November 2016. b) November 2017. Data ( $4 \text{ km}^2$  of resolution) were obtained from the official Giovanni Nasa site ([giovanni.gsfc.nasa.gov](http://giovanni.gsfc.nasa.gov)).

**Figura 7.** Distribución de clorofila-*a* ( $\text{mg}/\text{m}^3$ ) al sur del GSJ. a) Noviembre de 2016. b) Noviembre de 2017. Los datos ( $4 \text{ km}^2$  de resolución) fueron obtenidos del sitio oficial de Giovanni Nasa ([giovanni.gsfc.nasa.gov](http://giovanni.gsfc.nasa.gov)).

## DISCUSSION

Based on data from these two campaigns, the temperature records were  $0.5\text{-}1 \text{ }^\circ\text{C}$  higher than those previously described by Fernández et al. (2005) (Table 2). This is consistent with the previous observations on the variability of the system (Allega et al. 2021; Bodnariuk et al. 2021). On the other hand, salinity values (33.15 to 33.44) were lower than those described by Fernández et al. (2005) (33.48 to 33.66), but followed a similar pattern of variation (Table 2). Our results suggest that the density of the water column was governed by temperature as a consequence of the differences that have been mentioned in the values of temperature and salinity, the values of density were around  $0.25 \text{ kg}/\text{m}^3$  lower than those described by Fernández et al. (2005) (Table 2). This has as a direct consequence a strengthening of the stratification and an increase in the isolation between surface and deep waters with respect to previous years.

The pH values (7.70-8.19) were similar in magnitude to those presented by Torres et al. (2018) in 2016 for the entire gulf (7.5-8.2)

(Table 2), showing a characteristic pattern in which the values at the surface were spread more than near the bottom. This pattern could be explained since pH is closely related to the organisms that inhabit the environment through the carbon/carbonate balance, since the process of photosynthesis uses  $\text{CO}_2$  as a reagent for its reaction (Chen and Durbin 1994). In addition, the maximum pH values coincided with the maximum fluorescence values. This suggests there is an indirect relationship between pH and fluorescence or Chl-*a* as both are indirect indicators of phytoplankton biomass. It should be noted that the pH values changed from year to year and were higher when the water column was warmer (Table 2).

A large variability of macronutrient concentrations was observed, similar to those described by Akselman (1996) and Torres et al. (2018) for the entire SJG in the same season of the year. Torres et al. (2018) suggested that the vertical distribution of macronutrients was associated with the stability of the water column, which depends on the physical variables that regulate it. Likewise, our results showed that in the stations with stratified water column, nutrient concentrations at the surface were lower than near the bottom. In contrast, when the water column was homogeneous, the opposite was observed. The concentration at the surface increases and that near the bottom decreases because of mixing. In 2016, surface water showed a lower concentration of macronutrients in the north than in the southern half of the gulf (Torres et al. 2018). Although so far only  $\text{NO}_3^-$  was reported as a limiting nutrient for primary producers, in some stations measured during this work,  $\text{Si}(\text{OH})_4$  was also a limiting nutrient. Paparazzo et al. (2021) suggested that during the period studied (November 2016), when  $\text{NO}_3^-$  was low,  $\text{NH}_4^+$  played an important role for primary productivity due to the low water exchange in the column and the optimal relationship between preference and N availability in the environment. In addition, the authors discuss the type of primary production (new or regenerated) which depends on the least available nitrogen source. In addition to these observations, in this work we consider that, due to some observations of limiting  $\text{Si}(\text{OH})_4$ , biogenic silica should be measured to fully understand the distribution patterns observed by those authors.

A Si:N:P ratio (5.13:10.66:1) lower than that described by Redfield-Brzezinski (15:16:

**Table 2.** References of mean, standard deviation (SD), minimum (min) and maximum (max) between measurements of salinity, temperature (°C), density (kg/m<sup>3</sup>), pH, chlorophyll-*a* and nutrients (NO<sub>3</sub><sup>-</sup>, PO<sub>4</sub><sup>3-</sup> and Si(OH)<sub>4</sub>, μM) from this study and other studies during spring in the GSJ.

**Tabla 2.** Referencias de promedio (mean), desvío estándar (SD), mínimo (min) y máximo (max) entre las mediciones de salinidad, temperatura (°C), densidad (kg/m<sup>3</sup>), pH, clorofila-*a* y nutrientes (NO<sub>3</sub><sup>-</sup>, PO<sub>4</sub><sup>3-</sup> y Si(OH)<sub>4</sub>, μM) de este estudio y otros estudios durante primavera en el GSJ.

| Reference                          | Year | SJG area | Variable                           | Layer   | Mean  | SD   | Min   | Max   |
|------------------------------------|------|----------|------------------------------------|---------|-------|------|-------|-------|
| This work                          | 2016 | south    | Salinity                           | all     | 33.33 | 0.08 | 33.17 | 33.44 |
|                                    |      |          | Temperature (°C)                   | all     | 10.14 | 0.64 | 9.02  | 10.94 |
|                                    |      |          | Density (kg/m <sup>3</sup> )       | all     | 25.62 | 0.12 | 25.39 | 25.84 |
|                                    |      |          | pH                                 | all     | -     | -    | 7.70  | 8.12  |
|                                    |      |          | Chl- <i>a</i> (mg/m <sup>3</sup> ) | surface |       |      | 2.16  | 7.52  |
|                                    |      |          | NO <sub>3</sub> <sup>-</sup> (μM)  | all     | 8.32  | 5.71 | 1.45  | 14.92 |
|                                    |      |          | PO <sub>4</sub> <sup>3-</sup> (μM) | all     | 1.47  | 0.49 | 0.81  | 2.14  |
|                                    |      |          | Si(OH) <sub>4</sub> (μM)           | all     | 3.86  | 2.37 | 0.98  | 7.33  |
|                                    | 2017 | south    | Salinity                           | all     | 33.21 | 0.06 | 33.15 | 33.43 |
|                                    |      |          | Temperature (°C)                   | all     | 9.97  | 0.75 |       |       |
|                                    |      |          | Density (kg/m <sup>3</sup> )       | all     | 25.63 | 0.14 | 25.31 | 25.92 |
|                                    |      |          | pH                                 | all     | -     | -    | 7.79  | 8.19  |
|                                    |      |          | Chl- <i>a</i> (mg/m <sup>3</sup> ) | surface |       |      | 1.16  | 6.52  |
|                                    |      |          | NO <sub>3</sub> <sup>-</sup> (μM)  | all     | 7.44  | 4.61 | 0.02  | 15.50 |
| PO <sub>4</sub> <sup>3-</sup> (μM) |      |          | all                                | 1.57    | 0.42  | 0.80 | 2.48  |       |
| Si(OH) <sub>4</sub> (μM)           |      |          | all                                | 3.86    | 2.40  | 0.85 | 9.25  |       |
| Fernández et al. (2005)            | 1999 | all      | Salinity                           | bottom  | 33.59 | 0.10 | 33.26 | 33.69 |
|                                    |      |          | Temperature (°C)                   | bottom  | 9.10  | 0.79 | 8.04  | 11.43 |
|                                    |      |          | Density (kg/m <sup>3</sup> )       | bottom  | 25.99 | 0.16 | 25.47 | 26.18 |
|                                    |      |          | Chl- <i>a</i> (mg/m <sup>3</sup> ) | bottom  | 0.42  | 0.38 | 0.06  | 1.66  |
|                                    |      |          | Chl- <i>a</i> (mg/m <sup>3</sup> ) | surface | 0.57  | 0.40 | 0.10  | 2.21  |
|                                    |      | south    | Salinity                           | all     | 33.61 | 0.04 | 33.48 | 33.66 |
|                                    |      |          | Temperature (°C)                   | all     | 8.89  | 0.29 | 8.38  | 9.27  |
|                                    |      |          | Chl- <i>a</i> (mg/m <sup>3</sup> ) | bottom  | 0.26  | 0.10 | 0.03  | 0.63  |
|                                    |      |          | Chl- <i>a</i> (mg/m <sup>3</sup> ) | surface | 0.42  | 0.18 | 0.10  | 0.79  |
|                                    |      |          | pH                                 | all     | -     | -    | 7.50  | 8.20  |
| Torres et al. (2018)               | 2016 | all      | Chl- <i>a</i> (mg/m <sup>3</sup> ) | surface | ~4.00 |      |       |       |
|                                    |      |          | NO <sub>3</sub> <sup>-</sup> (μM)  | surface |       |      | 0.00  | 12.00 |
|                                    |      |          | PO <sub>4</sub> <sup>3-</sup> (μM) | surface |       |      | 0.40  | 1.60  |
|                                    |      |          | Si(OH) <sub>4</sub> (μM)           | surface |       |      | 1.00  | 5.00  |
|                                    |      |          | NO <sub>3</sub> <sup>-</sup> (μM)  | bottom  |       |      | 1.00  | 16.00 |
|                                    |      |          | PO <sub>4</sub> <sup>3-</sup> (μM) | bottom  |       |      | 1.00  | 2.50  |
|                                    |      |          | Si(OH) <sub>4</sub> (μM)           | bottom  |       |      | 1.80  | 11.00 |

1) is directly associated with the limitation in Si(OH)<sub>4</sub> and NO<sub>3</sub><sup>-</sup> discussed above. Sommer (1989) suggested that the nutrient requirements for each phytoplankton species are a key factor in regulating the composition of the phytoplankton community. Pappazzo et al. (2021) showed a great variation in the composition of the phytoplankton communities in the gulf. Although the adaptation of communities to changes in nitrogen sources is made clear, we consider that the availability of Si(OH)<sub>4</sub> could complement the interpretation of the system.

Our results showed high Chl-*a* concentration where nutrient concentration was low,

which could indicate nutrient uptake by phytoplankton. Phytoplankton blooms can be related to values above 1.5 mg/m<sup>3</sup> Chl-*a* (Treguer and Jacques 1992). Chl-*a* blooms, south of 45° S, start in late spring, early summer (November-January) (Romero et al. 2006). Based on remote sensing, Glembocki et al. (2015) showed a typical cycle for temperate regions of the annual Chl-*a*, when spring waters of SJG were stratified. This cycle was not observed in certain regions of the gulf, where the water column was not stratified, such as those mentioned in this study. Our results showed interannual variability of Chl-*a*, with concentrations (2.16-7.52 mg/m<sup>3</sup>) higher in 2016 than 2017 (1.16-6.52 mg/m<sup>3</sup>). Torres et

al. (2018) measured *in situ* Chl-*a* in 2016 and showed mean values of  $\sim 4.0$  mg/m<sup>3</sup>. Although the satellite Chl-*a* data are sufficiently robust to support our conclusions, when interpreting the results, it should be considered that A) the Chl-*a* concentration in the present work is a monthly average, B) there is a difference in MODIS algorithm performance by sampling location (Dogliotti et al. 2009), C) Williams et al. (2013) describe that the concentration obtained by MODIS-Aqua could overestimate *in situ* concentrations lower than 1.0 mg/m<sup>3</sup>, while underestimating concentrations higher than 1.0 mg/m<sup>3</sup>, in contrast to Dogliotti et al. (2009) which shows a general underestimation throughout the analyzed range of chlorophyll, and D) concentrations near the coast could be overestimated as there is the presence of suspended solids that could interfere with the satellite estimate (Romero et al. 2006; Williams et al. 2010).

Our results showed the presence of two types of fronts generated by different forcings in the south of the SJG. The presence of fronts could be identified when a water mass with a homogeneous water column meets a water mass with a marked stratification. This pattern was observed in the transects SE, SM, SW 2016 and in both SF. Our results show a consistent pattern of three layer in the stratified sector. The surface layer (mixed layer) showed relatively high temperature and low salinity, fluorescence, pH and nutrient concentration. In this layer, primary producers have adequate light conditions for their development. Macronutrients stimulate the growth of phytoplankton and were consumed until exhausted. When pycnocline develops, it isolates a bottom layer with low light availability, lower temperature and fluorescence and higher salinity and nutrients concentration than the surface. In contrast, in the homogeneous sector of the front, surface concentrations of macronutrients were higher and fluorescence was lower than the stratified region. This indicates that there was low nutrient uptake by primary producers due to the instability of the water column, which does not allow primary producers to be suspended in a surface layer where light is available. Due to the breakdown of stratification and the formation of the front, this injection of nutrients (from the homogeneous side of the front) would stimulate primary production in the stratified zone. Throughout the present study, the SJG showed spatial differences

associated with processes that generate the fronts and act on the physical, chemical and biological properties of the water.

The sector under study of the SJG was described as an area of coastal upwelling, both by numerical simulations (Tonini et al. 2006; Matano and Palma 2018) and through *in situ* measurements (Pisoni et al. 2020). Strong W-NW winds 48 h before our 2016 sampling generated the frontal conditions observed in our results. Paparazzo et al. (2021) showed that this upwelling generates a sudden change in nutrient availability and increase primary productivity. It was corroborated in our data in the SW and SM transects of 2016. On the contrary, during 2017 the winds were not favourable to break the stratification and the upwelling was not observed (Pisoni et al. 2020), and its consequence can be observed in our results for that year.

The SF transect crosses the thermohaline seasonal tidal front (Rivas and Pisoni 2010; Carbajal et al. 2018) located south of the SJG. Akselman (1996) and Glembocki et al. (2015) showed that its maximum development is observed in January. The monthly (November) SST satellite data showed a surface temperature gradient that indicates the presence of the front for both years, with the 2017 gradient higher than that of 2016. The surface presence of this thermal front could be observed through *in situ* data in 2017. However, in 2016 it was not possible to observe this front. Although, a thermal front was detected at the bottom, which makes us think that the surface front was still forming during our sampling and finished developing during the month of November.

Finally, in the SW 2017 transect, a low-salinity water intrusion ( $S < 33.25$ ) was observed in the subsurface. This water intrusion could be associated with the Magellanic plume entering the gulf via intermediate circulation, as described by Carbajal et al. (2018) and Palma et al. (2020). Our observations shows high nutrient concentration at station  $a_4$  (data not shown) and high subsurface fluorescence values (higher than expected) at 25 m. Carbajal et al. (2018) point out that in February, the low-salinity water plume provides nutrients and water with high concentrations of Chl-*a* during intermediate tide phase, which could explain the high fluorescence values. However, additional measures are needed to better understand this process.

## CONCLUSIONS

The southern sector of the SJG has different features depending on the external forces acting on it. Under certain wind conditions, an upwelling is generated in the coastal area. Additionally, the interaction of topography and tidal currents are conducive to the formation of fronts. The presence of fronts stimulates the growth of phytoplankton biomass through the injection of nutrients from well-mixed waters to stratified waters. This is observed during the austral spring, where the SJG shows high phytoplankton biomass. This paper provides direct information on how the physical and biogeochemical processes affect the productivity of this system.

**ACKNOWLEDGEMENTS.** We thank the San Jorge Gulf Working Group of the “Pampa Azul” initiative for providing the logistical framework for this work. In addition, thanks to the crew members of the R/V “Puerto Deseado” for their collaboration during the work on deck and to the Ba.R.D.O. (Base Regional de Datos Oceanográficos - Regional Oceanographic Data Base) for the processing of the CTD data. Thanks to the National Meteorological Service for the wind data. We also thank the official Giovanni Nasa website for allowing free access to the use of satellite images. Finally, we greatly appreciate the reviewers’ comments for helping to improve this paper.

## REFERENCES

- Acha, E. M., A. Piola, O. Iribarne, and H. Mianzan. 2015. Ecological processes on marine fronts: oases in the ocean. 1ra Edición. Springer. Mar del Plata, Buenos Aires, Argentina. <https://doi.org/10.1007/978-3-319-15479-4>.
- Akselman, R. 1996. Estudios ecológicos en el Golfo San Jorge y adyacencias (Atlántico Sudoccidental). Distribución, abundancia y variación estacional del fitoplancton en relación a factores físico-químicos y la dinámica hidrológica. Universidad de Buenos Aires.
- Allega, L., J. P. Pisoni, E. Cozzolino, R. A. Maenza, and M. C. Piccolo. 2021. The variability of sea surface temperature in the Patagonian Shelf Argentina, from 35 years of satellite information. *International Journal of Remote Sensing* 42(16):6090-6106. <https://doi.org/10.1080/01431161.2021.1934600>.
- Belkin, I. M., and J. E. O'Reilly. 2009. An algorithm for oceanic front detection in chlorophyll and SST satellite imagery. *Journal of Marine Systems* 78(3):319-326. <https://doi.org/10.1016/j.jmarsys.2008.11.018>.
- Bianchi, A. A., L. Bianucci, A. R. Piola, D. R. Pino, I. Schloss, A. Poisson, and C. F. Balestrini. 2005. Vertical stratification and air-sea CO<sub>2</sub> fluxes in the Patagonian shelf. *Journal of Geophysical Research: Oceans* 110(C7). <https://doi.org/10.1029/2004JC00248>.
- Bianchi, A. A., D. R. Pino, H. G. I. Perlender, A. P. Osiroff, V. Segura, V. Lutz, and A. R. Piola. 2009. Annual balance and seasonal variability of sea-air CO<sub>2</sub> fluxes in the Patagonia Sea: Their relationship with fronts and chlorophyll distribution. *Journal of Geophysical Research: Oceans* 114(C3). <https://doi.org/10.1029/2008JC004854>.
- Bodnariuk, N., C. G. Simionato, and M. Saraceno. 2021. SAM-driven variability of the southwestern Atlantic shelf sea circulation. *Continental Shelf Research* 212:104313. <https://doi.org/10.1016/j.csr.2020.104313>.
- Brzezinski, M. A. 1985. The Si: C: N ratio of marine diatoms: interspecific variability and the effect of some environmental variables. *Journal of Phycology* 21(3):347-357. <https://doi.org/10.1111/j.0022-3646.1985.00347.x>.
- Carbajal, J. C., A. L. Rivas, and C. Chavanne. 2018. High-frequency frontal displacements south of San Jorge Gulf during a tidal cycle near spring and neap phases: Biological implications between tidal states. *Oceanography* 31(4): 60-69. <https://doi.org/10.5670/oceanog.2018.411>.
- Chen, C. Y., and E. G. Durbin. 1994. Effects of pH on the growth and carbon uptake of marine phytoplankton. *Marine Ecology-Progress Series* 109:83-94. <https://doi.org/10.3354/meps109083>.
- Costanza, R., R. d'Arge, R. De Groot, S. Farber, M. Grasso, B. Hannon, K. Limburg, S. Naeem, R. V. O'Neill, J. Paruelo, R. G. Raskin, P. Sutton, and M. van den Belt. 1997. The value of the world's ecosystem services and natural capital. *Nature* 387:253-260. <https://doi.org/10.1038/387253a0>.
- Dogliotti, A. I., I. R. Schloss, G. O. Almandoz, and D. A. Gagliardini. 2009. Evaluation of SeaWiFS and MODIS chlorophyll-a products in the Argentinean Patagonian Continental Shelf (38° S-55° S). *International Journal of Remote Sensing* 30(1):251-273. <https://doi.org/10.1080/01431160802311133>.
- Fernández, M., J. I. Carreto, J. Mora, and A. Roux. 2005. Physico-chemical characterization of the benthic environment of the Golfo San Jorge, Argentina. *Journal of the Marine Biological Association of the United Kingdom* 85:1317-1328. <https://doi.org/10.1017/S002531540501249X>.
- Fernández, M., D. Cucchi-Colleoni, A. Roux, Á. Marcos, and E. Fernández. 2007. Caracterización físico-química del sistema bentónico en el sector sur del Golfo San Jorge, Argentina. *Revista de Biología Marina y Oceanografía* 42(2): 177-192. <https://doi.org/10.4067/S0718-19572007000200005>.
- Flores-Melo, X., I. R. Schloss, C. Chavanne, G. O. Almandoz, M. Latorre, and G. A. Ferreyra. 2018. Phytoplankton ecology during a spring-neap tidal cycle in the southern tidal front of San Jorge Gulf, Patagonia. *Oceanography* 31(4): 104-112. <https://doi.org/10.5670/oceanog.2018.412>.
- Glembocki, N. G., G. N. Williams, M. E. Góngora, D. A. Gagliardini, and J. M. Orensanz. 2015. Synoptic oceanography of San Jorge Gulf (Argentina): A template for Patagonian red shrimp (*Pleoticus muelleri*) spatial dynamics. *Journal of Sea Research* 95:22-35. <https://doi.org/10.1016/j.seares.2014.10.011>.

- Góngora, M. E., D. González-Zevallos, A. Pettovello, and L. Mendía. 2012. Caracterización de las principales pesquerías del golfo San Jorge Patagonia, Argentina. *Latin American Journal of Aquatic Research* 40(1):1-11. <https://doi.org/10.3856/vol40-issue1-fulltext-1>.
- Guerrero, R. A., and A. R. Piola. 1997. Masas de agua en la plataforma continental. *El Mar Argentino y sus Recursos Pesqueros* 1:107-118. <http://hdl.handle.net/1834/1703>.
- Laurs, R. M., P. C. Fiedler, and D. R. Montgomery. 1984. Albacore tuna catch distributions relative to environmental features observed from satellite. *Deep-Sea Research* 31:1085-1099. [https://doi.org/10.1016/0198-0149\(84\)90014-1](https://doi.org/10.1016/0198-0149(84)90014-1).
- Matano, R. P., and E. D. Palma. 2018. Seasonal variability of the oceanic circulation in the Gulf of San Jorge, Argentina. *Oceanography* 31(4):16-24. <https://doi.org/10.5670/oceanog.2018.402>.
- Millero, F. J. 2005. *Chemical oceanography*. 3<sup>rd</sup> edition. Pp. 536. Boca Raton, CRC Press. <https://doi.org/10.1201/9780429258718>.
- NASA. 2018. Goddard Space Flight Center, Ocean Ecology Laboratory, Ocean Biology Processing Group. Moderate-resolution Imaging Spectroradiometer (MODIS) Aqua Chlorophyll Data. NASA OB DAAC, Greenbelt, MD, USA.
- Olson, D. B. 2002. Biophysical dynamics of ocean fronts. Pp. 187-218 *in* A. R. Robinson, J. J. McCarthy and B. Rothschild (eds.). *Biological-Physical Interactions in the Sea*. The Sea 12.
- Paparazzo, F. E. 2003. Evaluación de nutrientes inorgánicos en aguas oceánicas y su relación con la biomasa fitoplanctónica. Tesis de licenciatura en Ciencias Biológicas. Universidad Nacional de la Patagonia San Juan Bosco Facultad de Ciencias Naturales Sede Puerto Madryn.
- Paparazzo, F. E., R. Pierattini-Martínez, E. Fabro, R. J. Gonçalves, A. C. Crespi-Abril, G. R. Soria, E. S. Barbieri, and G. O. Almandoz. 2021. Relevance of sporadic upwelling events on primary productivity: The key role of nitrogen in a gulf of SW Atlantic Ocean. *Estuarine, Coastal and Shelf Science* 249:107123. <https://doi.org/10.1016/j.ecss.2020.107123>.
- Pisoni, J. P., A. L. Rivas, and M. H. Tonini. 2020. Coastal upwelling in the San Jorge Gulf (Southwestern Atlantic) from remote sensing, modelling and hydrographic data. *Estuarine, Coastal and Shelf Science* 245:106919. <https://doi.org/10.1016/j.ecss.2020.106919>.
- Redfield, A. C. 1934. On the proportions of derivatives in sea water and their relation to the composition of plankton. Pp. 176-192 *in* R. J. Daniel (ed.). *James Johnstone Memorial Volume I*. Liverpool: University of Liverpool. UK.
- Rivas, A. L., and J. P. Pisoni. 2010. Identification, characteristics and seasonal evolution of surface thermal fronts in the Argentinean Continental Shelf. *Journal of Marine Systems* 79(1-2):134-143. <https://doi.org/10.1016/j.jmarsys.2009.07.008>.
- Romero, S. I., A. R. Piola, M. Charo, and C. A. Eiras Garcia. 2006. Chlorophyll-a variability off Patagonia based on SeaWiFS data. *Journal of Geophysical Research: Oceans* 111:1-11. <https://doi.org/10.1029/2005JC003244>.
- Skalar Analytical® V. B. 2005a. Skalar Methods - Analysis: Nitrate + Nitrite - Catnr. 461-031 + DIAMOND Issue 081505/MH/99235956. Breda (The Netherlands).
- Skalar Analytical® V. B. 2005b. Skalar Methods - Analysis: Phosphate - Catnr. 503-010w/r + DIAMOND Issue 081505/MH/99235956. Breda (The Netherlands).
- Skalar Analytical® V. B. 2005c. Skalar Methods - Analysis: Silicate - Catnr. 563-051 + DIAMOND Issue 081505/MH/99235956. Breda (The Netherlands).
- Svensden, G. M., M. O. Reinaldo, M. A. Romero, G. Williams, A. Magurran, S. Luque, and R. A. González. 2020. Drivers of diversity gradients of a highly mobile marine assemblage in a mesoscale seascape. *MEPS* 638:149-164. <https://doi.org/10.3354/meps13264>.
- Sommer, U. 1989. The Role of Competition for Resources in Phytoplankton Succession. Pp. 57-106 *in* U. Sommer (ed.). *Plankton Ecology*. Brock/Springer Series in Contemporary Bioscience. Springer, Berlin, Heidelberg. [https://doi.org/10.1007/978-3-642-74890-5\\_3](https://doi.org/10.1007/978-3-642-74890-5_3).
- Tonini, M., E. D. Palma, and A. L. Rivas. 2006. Modelo de alta resolución de los golfos patagónicos. *Mecánica Computacional* 25:1441-1460.
- Torres, A., F. E. Paparazzo, G. N. Williams, A. L. Rivas, M. Solis, and J. L. Esteves. 2018. Dynamics of Macronutrients in the San Jorge Gulf during spring and summer. *Oceanography* 31:25-32. <https://doi.org/10.5670/oceanog.2018.407>.
- Tréguer, P. J., and G. Jacques. 1992. Dynamics of nutrients and phytoplankton, and fluxes of carbon, nitrogen and silicon in the Antarctic Ocean. *Polar Biology* 12:149-162. <https://doi.org/10.1007/BF00238255>.
- Williams, G. N., A. I. Dogliotti, P. Zaidman, M. Solis, M. A. Narvarde, R. C. Gonzalez, J. L. Esteves, and D. A. Gagliardini. 2013. Assessment of remotely-sensed sea-surface temperature and chlorophyll-a concentration in San Matías Gulf (Patagonia, Argentina). *Continental Shelf Research* 52:159-171. <https://doi.org/10.1016/j.csr.2012.08.014>.
- Williams, G., M. Sapoznik, M. Ocampo-Reinaldo, M. Solis, M. Narvarde, R., González, and D. Gagliardini. 2010. Comparison of AVHRR and SeaWiFS imagery with fishing activity and in situ data in San Matías Gulf, Argentina. *International Journal of Remote Sensing* 31(17-18):4531-4542. <https://doi.org/10.1080/01431161.2010.485218>.
- Yañez, E., V. Catasti, M. A. Barbieri, and G. Böhm. 1996. Relaciones entre la distribución de recursos pelágicos pequeños y la temperatura superficial de la mar registrada con satélites NOAA en la zona central de Chile. *Investigaciones Marinas*. Valparaíso 24:107-122. <https://doi.org/10.4067/S0717-71781996002400009>.